

## CHARACTERIZATION TECHNIQUES TO VALIDATE MODELS OF DENSITY VARIATIONS IN PRESSED POWDER COMPACTS

Terry Garino\*, Mike Mahoney\*, Mike Readey\*, Kevin Ewsuk\*,  
John Gieske\*, Gerry Stoker\* and Shermann Min†

Sandia National Laboratories

\*Albuquerque, NM 87185

†Livermore, CA

### ABSTRACT

In this study, techniques for characterizing density gradients generated during typical powder compaction processes are reviewed and several are evaluated. The techniques reviewed are ultrasonic velocity measurements, laser ultrasonic velocity measurements, x-ray radiography, autoradiography, computed tomography (CT), magnetic resonance imaging (MRI), and simple image analysis of polished cross-sections. Experimental results are reported for all of these techniques except autoradiography, CT and MRI. The test specimens examined were right circular cylinders of a high length/diameter ratio (to ensure significant density variation) pressed from commercial spray-dried alumina powders. Although the density gradients could be detected with all four techniques, ultrasonic velocity measurements gave the best contour map of gradients and is therefore most suitable for model validation. On the other hand, it was concluded that x-ray radiography is preferable in situations where cost and/or number of samples are more important than high resolution.

KEY WORDS: Characterization, Density Gradients, Powder Compacts

*OG*  
DISTRIBUTION OF THIS DOCUMENT IS UNLIMITED

MASTER

## **DISCLAIMER**

**Portions of this document may be illegible in electronic image products. Images are produced from the best available original document.**

# 1. INTRODUCTION

It is widely recognized that during the die pressing of powders, considerable variation in density develops due to the influence of die wall friction (1). In ceramics, density variations are typically manifest during sintering, i.e, the gradients in green density lead to non-uniform shrinkage. This in turn often necessitates costly hard-tool grinding to achieve the desired component dimensions. Over the past 100 years or so, much attention has been directed towards modeling the influence of die wall friction and its resultant effect on density distributions in pressed powder compacts. As a result, a plethora of models now exist to describe the response of powders under a consolidating pressure in a die cavity. The models range from rather simple to extremely complex, depending on the constitutive laws used to describe the powder assembly: as elastic, plastic, or viscoelastic continua. Yet they all have one trait in common, namely that they all predict the same general trends in the spatial variability of density. Unfortunately, there is little experimental evidence to indicate which models, if any, accurately describe the density gradients in a powder compact. In order to validate existing or improved compaction models, it is important to be able to accurately measure density gradients that are generated during typical green body consolidation processes. Characterization of density gradients is also important in industrial settings where mold design and other factors may change frequently. In this setting, cost and throughput of samples may be more important than high resolution.

Density gradients in pressed ceramic powder compacts can be characterized using a variety of different techniques. Each technique has its own advantages and disadvantages relating to performance and cost. The major factors considered important for performance are accuracy and sensitivity of density measurements, spatial resolution, speed of measurement, amount of sample preparation required, and ease of interpreting the data. In this section, a number of characterization techniques will be reviewed. The reviews include a brief discussion of how each technique works and its relative advantages and disadvantages.

## 2. REVIEW OF CHARACTERIZATION TECHNIQUES

**2.1 Ultrasonic Velocity Measurements** One method of characterizing density gradients in green ceramics utilizes ultrasonic velocity measurements, a technique that is commonly used in a variety of non-destructive evaluation applications. With this technique, the density of a material is indirectly determined from the velocity of an ultrasonic pulse moving through the material (2). The pulses are produced by a transducer, usually a piezoelectric, which is scanned across the surface of the sample. Generally a frequency of several MHz is used along with a longitudinal wave mode. Each pulse is detected with another transducer either after a single pass through the material or after one or more reflections off of the surfaces. From the local sample thickness and the time between the sending of the pulse and its detection, the ultrasonic velocity can be obtained. In practice, it is convenient for the sample to have two flat parallel surfaces, perpendicular to which the pulses move so that the

thickness does not have to be measured at every point where a velocity measurement is made.

The relationship between the ultrasonic velocity and the properties of the material for a longitudinal wave is given by

$$v = \sqrt{\frac{E(1-\nu)}{\rho(1+\nu)(1-2\nu)}} \quad [1]$$

where  $\rho$  is the density of the material,  $E$  is the Young's modulus and  $\nu$  is the Poisson's ratio. While the Poisson's ratio is only slightly density dependent, the Young's modulus is a strong function of the relative density of a material so that the velocity increases with decreasing porosity. Moreover, no universal relationship between Young's modulus and relative density exists that applies to all materials, so that a calibration curve needs to be constructed using measurements on samples of the same material that have uniform and independently measurable densities in the range of interest. Using the calibration curve and the velocities measured by scanning the entire sample, a contour map of the sample can be constructed that shows the density as a function of position. With a good ultrasonic system, density measurements can be made with the accuracy and sensitivity on the order of a few tenths of a per cent. Units to perform this type of characterization are commercially available but those capable of determining density gradients with adequate resolution are relatively expensive. Determining the spatial resolution is somewhat complicated since the data is produced by scanning a relatively large probe (5 to 15 mm in diameter) across the sample with small steps, but is generally on the order of several tenths of a mm. With an automated system, scanning a sample takes on the order of an hour or less. As with other characterization techniques, analysis of composite ceramic compacts, such as silicon carbide whiskers in alumina powder or alumina/zirconia powder mixtures, is difficult since compositional gradients will affect the velocities measured in addition to porosity gradients.

To use ultrasonic velocity measurements to characterize the density gradients in a pressed ceramic powder compact, a suitable sample geometry must first be selected. For example, for a typical right circular cylinder, a longitudinal slab cut from the center of the cylinder will contain all of the density gradients present because of the circular symmetry of the cylinder, assuming that the gradients are due to die wall and interparticle friction and are not caused by non-uniform die fill. However this type of sample geometry, although convenient for this and several of the other characterization techniques, introduces a spatial resolution problem due to the finite thickness of the slab since the regions of constant density are curved due to the circular symmetry. The situation is the worst at the longitudinal axis of the slab since the pulse, or any other probe such as an x-ray, will pass through material whose density varies from that at the center to that at a distance of half of the slab thickness from the center. Therefore, the spatial resolution is maximized by decreasing the thickness of the slab. This is illustrated in Figure 1 for slabs of three different thicknesses, 1, 3 and 5 mm, cut from a 30 mm diameter cylinder. As shown in the figure, the resolution starts at half the slab thickness and then decreases such that the ratio of the resolutions for slabs of two different thicknesses approaches the ratio of the squares of the thicknesses at distances from the center several times the thickness of the thinner slab. The figure also shows that a

thickness of 1 mm should be adequate for most situations since the resolution is better than 0.1 mm for distances greater than about 1 mm from the center. Fabricating such a thin slab may require that the compact be bisque fired to increase the strength without altering the density distribution significantly. Since the velocity is a strong function of density at low densities, it is critical that the compact and the samples used for calibration be bisque fired identically.

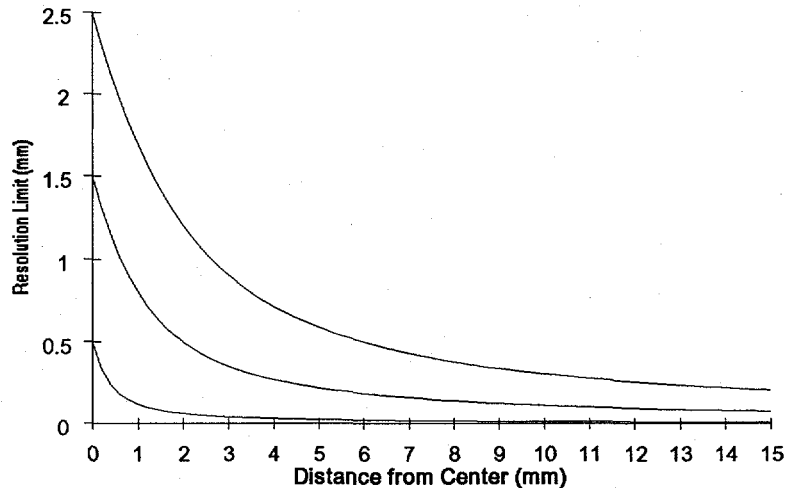


Figure 1. The effect of slab thickness on spatial resolution for three slab thicknesses, 5 mm (top curve), 3 mm (middle curve) and 1 mm.

For ultrasonic evaluation, a porous sample is generally immersed in a liquid such as water or ethanol to improve the coupling between the transducer and the sample. Bisque firing can be used so that the liquid will not cause the compact to swell and/or disintegrate. However, several techniques for dry coupling to porous ceramic samples have been reported. Wright, et. al. (3), used a thick layer of a silicone gel between the transducer and their silicon nitride sample, which they did not want to contaminate by liquid immersion. Other non-immersion coupling techniques include the use of a novel elastomer material by Jones, et. al. (4), a vacuum sealed polymer membrane by Roberts (5) and adhesive tape by Yamanaka, et. al (6).

**2.2 Laser Ultrasonics** A relatively new non-contact, non-destructive evaluation technique similar to conventional ultrasonics is laser ultrasonics (LU), a technique in which elastic waves are both generated and detected optically. Typically, a high-power laser pulse is directed at the sample to induce stress waves. The opto-acoustic method by which these waves are produced is different depending on the energy of the laser pulse (7). In the thermoelastic region, waves are generated due to the sudden local expansion that accompanies the temperature increase in the region where the laser strikes the sample. At higher laser energies, ablation (i.e. plasma formation/dielectric breakdown) can occur. In this case, material is ejected from the surface causing a shock wave (which weakens into an

elastic wave) to propagate into the sample. Unlike the thermoelastic region, where the sample, upon cooling, remains the same, ablation can leave a visible pit of perhaps a few microns in depth. When a single laser pulse is used as the source, essentially all wave modes that can be supported by the sample are produced. That is longitudinal, shear, Lamb and surface waves are generated simultaneously and can complicate the analysis of the acquired waveforms. Detection may be accomplished via optical interferometry that utilizes a second illumination laser. The main benefit of using a fully optical system over conventional transducers is the ability to direct laser beams within hostile (e.g. a furnace) or unaccommodating (e.g. moving surfaces) environments. Since an energy couplant is not needed for the transduction process, LU is ideal for process monitoring and in-situ material characterization. The use of this technique to characterize green ceramics has been reported by Oksanen, et al (8).

**2.3 X-ray Radiography** X-ray radiography refers to another non-destructive evaluation technique in which a uniform x-ray beam is directed through a sample, which attenuates the beam depending on its composition and the presence of defects such as pores, onto a film, for example, that records a two dimensional image of the intensity distribution produced by the sample (9). For application to determining density gradients in ceramic compacts, the intensity of x-rays passing through a region of the sample will be dependent on the product of the sample thickness and the relative density of that according to Beer's Law. Typically, x-ray radiography is performed using commercially available, moderately priced systems that are suitable for determining density gradients in pressed powder compacts. These units produce x-rays with a distribution of wavelengths with a maximum energy that can be controlled. The slab geometry described above is also suitable for this technique. The x-ray energy and the exposure time need to be adjusted, depending on the sample thickness and composition, to produce a film image with the optimum contrast between regions of high and low density. Generally, the highest density sensitivity is achieved with the lowest energy x-rays that can be practically used, usually between 10 and 50 KV. This fact is simply a consequence of Beer's Law.

The transmitted intensity variations are usually recorded on film, although it is possible to directly record the image electronically using a CCD camera. Once such an image is produced, some method must be used to correlate the relative densities with the various shades of gray on the film or electronic image. This can be accomplished by radiographing the unknown sample along with a calibration sample uniform density close to the density of the sample. The calibration standard should be machined to form a step wedge having step thickness centered on that of the sample. If film is used, the optical density of the film can be measured with an optical densitometer or they can be transformed into electronic images with an optical scanner. The electronic images, either from the camera or the scanner, can then be manipulated using a computer with appropriate software such as Adobe Photoshop to, for example, increase the contrast. Regions on the test sample image can then be assigned densities by comparison with the different thickness sections on the calibration standard image. The spatial resolution obtained depends on several factors. If an optical densitometer is used, the resolution is set by the size of its aperture, typically on the order

of 1 mm. For the electronic images, the resolution is set by the resolution of the camera or scanner.

Two significant advantages of using x-ray radiography for characterizing density gradients in ceramic compacts are that bisque firing is not necessary unless it is required for sample preparation and that a relatively large number of samples can be characterized simultaneously. Analysis of composite materials is difficult but may be possible by utilizing a variety of different energies. There are also several disadvantages to this technique. The sensitivity of the density measurement is on the order of a per cent and decreases with decreasing sample thickness, so that for longitudinal slab samples, the spatial resolution and the density sensitivity vary in opposite ways with thickness. A thickness of several mm is required to achieve a density sensitivity of one per cent. Another potential problem is caused by the scattering of the x-rays which affects the sharpness of the image at the sample edges. When primary x-rays strike any object in the system, low energy x-rays are produced by scattering that travel in directions not necessarily parallel to the primary x-rays. Thus, some of these scattered x-rays will just miss the edge of the sample at such an angle that they will strike the film in a region inside of the actual edge of the sample producing a darker image in this region. This effect can be minimized by placing a metal foil over the sample to block out the low energy x-rays.

**2.4 Autoradiography** A technique similar to x-ray radiography that has been used to characterize density gradients in pressed ceramic compacts is autoradiography. In this technique, the sample is itself radioactive. When placed directly on a film the sample forms an image with gray levels proportional to local densities. This technique can be made applicable to materials that are not radioactive by "labeling" the particles of the material with a radioactive isotope. Use of radioactive materials is a disadvantage of this technique since in either case radioactive materials must be handled and then disposed of. Total imaging time can be rather long due to the low level of energy emitted.

Autoradiography was used by MacLeod and Marshall (10) in one of the few studies that characterized the density gradients in pressed ceramic powder compacts. They used a natural enrichment grade of uranium dioxide. Longitudinal slices cut from cylindrical compacts produced at various pressures, aspect ratios, etc., were placed directly on fine-grained x-ray film under a 100g weight and exposed for 24 hr. An optical densitometer with a 1.0 by 0.5 mm aperture was then used to measure the optical density of the exposed film at points on a 3 mm grid. These values were converted to relative density values using a calibration curve produced by measuring the optical density of images of a series of samples with different, uniform densities. From this data, they constructed contour maps of the samples with a density sensitivity of several tenths of a per cent.

**2.5 X-ray and  $\gamma$ -ray Computed Tomography** Computed tomography is a non-destructive evaluation technique that can be applied to the characterization of density gradients in ceramic compacts without the need for any sample preparation (11). CT can be done with either x-rays or  $\gamma$ -rays, which are higher energy radiation produced by radioactive isotopes such as  $^{60}\text{Co}$  and  $^{192}\text{Ir}$ . For simplicity, the use of x-rays will be assumed in the

following discussion although the process is the same for  $\gamma$ -rays. CT is accomplished by first scanning a narrow, collimated x-ray beam across the object while measuring the intensity of the transmitted x-rays with an x-ray detector, and then repeating this process after the object (or the x-ray source and detector) is moved in small angular increments through  $180^\circ$ . The intensity profiles obtained at each angle, called projections, are stored in a computer. The computer then processes the projection data and reconstructs the amount of x-ray attenuation produced by each small volume element, or voxel, in the object. The reconstruction can be performed using one of several techniques including iterative techniques, back-projection methods and the Fourier transforms method. The attenuation values calculated for the voxels are then assigned various shades of gray (or colors) so that an image of a plane of voxels, a tomogram, can be constructed where the gray level of a voxel is proportional to the density of the material to which it corresponds. To quantify the gray levels in a tomogram of a ceramic compact that contains density gradients, several compacts of the same material that each have different, uniform densities should be tomographed along with the sample compact.

$\gamma$ -ray CT has several advantages over x-ray CT (12). Since the energy of  $\gamma$ -rays is higher, thicker samples can be characterized. Also, since radioactive isotopes produce either monochromatic or a well-defined spectrum of photons, beam-hardening artifacts caused by the larger attenuation of the lower energy photons in a polychromatic beam either does not occur or can be corrected for exactly. Finally, since the photon spectrum is simple, absolute density values can be directly determined without the need for calibration standards by using the attenuation coefficients of the material at the one or well-defined spectrum of wavelengths of the photons used.

In addition to not requiring any sample preparation, computed tomography has several other advantages. Tomograms of any number of planes in the sample can be created. The density sensitivity is about 0.2% and the spatial resolution is in the range of 0.4 to 1 mm. The major disadvantage is the cost of the CT unit. Also, depending on the shape of the object, it may be necessary to immerse the sample in a modifying liquid to suppress partial volume artifacts. This is due to the abrupt change in x-ray attenuation that occurs at an edge if the sample is in air and is especially a problem for high aspect ratio samples.

X or  $\gamma$ -ray have been used in several studies to characterize density gradients in green ceramics. Rokugawa, et. al. (12), used  $\gamma$ -ray CT to examine injection molded silicon nitride punch guides and valves and  $\beta$ -Sialon nozzles. They found that all of the parts were quite uniform with density variations comparable to the noise level, 0.25 to 1.0%. Ellingson, et. al. (13), used microfocus x-ray CT to examine green or presintered silicon carbide whisker/silicon nitride composites for by pressure-slip-casting. In all cases that the density was observed to decrease from the edge of the cylindrical samples to the center.

**2.6 Magnetic Resonance Imaging** Magnetic resonance imaging (MRI) is a non-destructive analysis technique that is similar to CT in that it is capable of producing images of planes in an object (14). For MRI, the image is related to the nuclear magnetic

resonance (NMR) signal produced by each volume element in the image plane of the sample. NMR is a quantum effect, the details of which are beyond the scope of this paper. To apply MRI to characterizing density gradients in ceramic compacts, the pores in the compact must be filled with a liquid that produces a strong NMR signal so that the intensity of a region of the image will be proportional to the concentration of the liquid and thus to the porosity in that region. Therefore, the liquid must completely fill all of the pores in the compact. Complete filling is promoted using vacuum impregnation and by choosing a low viscosity liquid that has a low interfacial tension with the sample material. To produce a strong NMR signal, the filler liquid must contain an isotope, hopefully in high concentration, that has high sensitivity such as  $^1\text{H}$ , the highest sensitivity isotope, or  $^{19}\text{F}$ , which is 80% as sensitive as hydrogen. Also, a simple NMR spectrum is desirable which results from a molecular structure with a high degree of chemical symmetry. Some examples of good filler liquids are water, benzene and acetone (15).

There are two relaxation times associated with NMR that have large impact on MRI. The first is the spin-lattice relaxation time,  $T_1$ , which is the characteristic time for the buildup of magnetic polarization of a nucleus.  $T_1$  controls the rate that NMR data can be acquired in the image forming process. Doping the filler liquid with a paramagnetic substance lowers  $T_1$  by about an order of magnitude leading to a similar decrease in the total imaging time and a similar increase in the signal to noise ratio per unit time. The spin-spin relaxation time,  $T_2$ , is related to the decay time of the NMR signal and affects both the spatial resolution and the signal to noise ratio. Both of these factors improve with increasing  $T_2$ .

The advantages of MRI include the ability to image a variety of planes using an intact sample with good density (<1%) and spatial (0.3 mm) resolution in a reasonably short time if a paramagnetic dopant is used. Disadvantages include the high cost of an MRI system and the need to infiltrate the samples with a liquid.

The use of MRI to characterize ceramic powder compacts was studied by Ellingson, et. al (15). They used benzene as the filler liquid with chromium acetylacetonate as the paramagnetic dopant. They found that MRI was capable of imaging density gradients in green and bisque-fired compacts of alumina, magnesium oxide and silicon carbide.

**2.7 Image Analysis** In this technique, two dimensional images (usually generated by optical or electron microscopy) are digitized and converted into a binary image (black and white) using gray scale thresholding common to image processing software. From the binary image, an areal fraction of either binary phase can be quantified. In the case of pressed powder compacts containing a significant fraction of porosity, the binary image represents porosity and the ceramic particles. Also, pressed powder compacts must be impregnated with epoxy or a similar material so that images suitable for analysis can be obtained.

Density maps are then obtained by imaging several regions of axial or longitudinal cross-sections of the powder compacts. The areal fraction of solid phase (i.e., the relative density) can then be plotted as a function of axial and radial position within the sample. An

advantage of this technique is the high spatial resolution obtainable using an SEM. Disadvantages include cost and speed, especially if a contour map of an entire sample is desired.

### 3. EXPERIMENTAL

Nearly all of the techniques described above are being evaluated to compare their ability to characterize density gradients in uniaxially pressed ceramic powder compacts. Work is ongoing using the following techniques: ultrasonic velocity measurement, laser ultrasonics, x-ray radiography, x-ray CT, MRI and image analysis. Preliminary results for all of these techniques except x-ray CT and MRI will be reported.

**3.1 Sample Preparation** Samples for density gradient characterization were prepared by uniaxially pressing a spray-dried 94% alumina powder containing a methylcellulose binder in a 2.22 cm (0.875 in) diameter die at 68.9 MPa (10 Ksi). The pressed compacts had aspect ratios of about 1.6, which is large enough so that significant density gradients were expected. The overall green density of the compacts was 52%. Some compacts were bisque fired by heating at 10°C/min to 1300°C and holding for 10 min. Longitudinal slices were cut from the compacts with a diamond saw and then milled to a desired thickness with flat, parallel surfaces. For the x-ray radiography experiments, step wedge calibration standards with five steps were fabricated from the same alumina powder pressed in large diameter die at 68.9 MPa. The center step was the same thickness as the sample slice and there was a 5% difference in thickness between successive steps. The density of the wedge was 54%. For the ultrasonic velocity measurements, standards were fabricated by pressing the same alumina powder into low aspect ratio compacts at 34.5, 68.9, 103.4 and 137.8 MPa to produce densities ranging from 50% to 56%.

**3.2 Ultrasonic Velocity Measurements** An ultrasonic velocity image map of the sample was created scanning the sample in the pulse-echo mode at 5 MHz with a 5 mm transducer. The sample was immersed in 95% ethanol to aid in coupling. The pulse-echo waveform was digitized at a 200 MHz rate and was recorded at 0.2 mm increments using the Sandia high precision ultrasonic data acquisition and display system. The time-of-flight (TOF) for the pulse to travel through twice the thickness of the sample was calculated at each transducer position and its value was displayed according to a pseudocolor scale. The ultrasonic velocity in the sample for each color was calculated by dividing twice the thickness by the measured TOF. The color scale for velocity was calibrated for density by performing similar measurements on the standards.

A map of the ultrasonic velocities measured for the sample is shown in Figure 2. Density values were assigned to the scale below the map based on the results of the measurements on the standards. The shade of gray in the bottom corners corresponds to the shade in the scale just below 50% density. The map shows that the density increases from about 49% in

the bottom corners to 56% in the upper corners with a symmetric distribution about the center

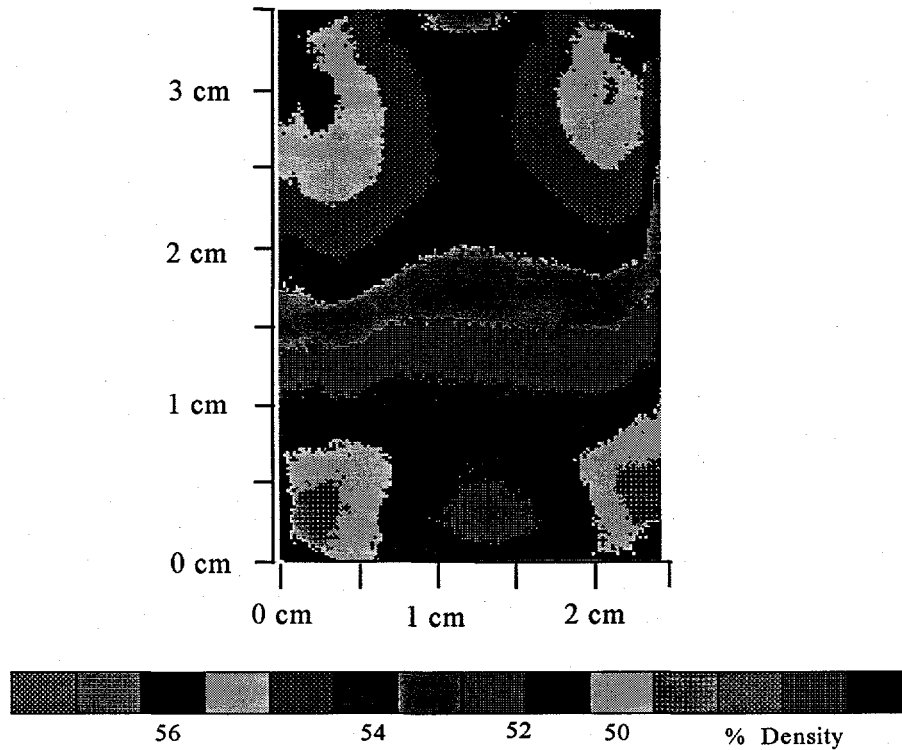


Figure 2. Density contour map of a 5 mm thick slab of an alumina compact pressed at 68.9 MPa derived from ultrasonic velocity measurements. The shade of gray near the bottom corners corresponds to about 49%.

line. Along the center line the density increases from 52% to 54% from bottom to top. These trends are consistent with expectations since due to die-wall friction the effective pressure decreases from top to bottom. As indicated on the scale, the relation between velocity and density is non-linear so that the resolution increases from about 1% at low density to almost 0.5% at high density.

**3.3 Laser Ultrasonics** Laser ultrasonic velocity measurements were made on bisque-fired samples. A frequency-doubled, Q-switched Nd:YAG laser was used to generate Rayleigh waves. Detection was performed with a 200 mW diode-pumped CW illumination laser in conjunction with a confocal Fabry-Perot interferometer. This detection technique was chosen because of its ability to accommodate diffusely reflecting surfaces (no surface preparation was needed). The generation laser was focused to a  $\sim 5$  mm x 0.2 mm line while the detection beam was focused to a  $\sim 0.2$  mm diameter spot which was directed several millimeters away from the generation beam on the same side of the sample. The generation laser's pulse width was 20 ns and the energy ( $< 2$  mJ per pulse) was near the threshold for ablation.

The results of laser ultrasonic velocity measurements taken at 5 mm intervals along lines near the edges and along the center of the sample are given in Figure 3. The trends shown in the figure are consistent with the results from conventional ultrasonics in that there is about a 10% decrease in velocity from top to bottom along the edges and a significantly smaller decrease along the center line.

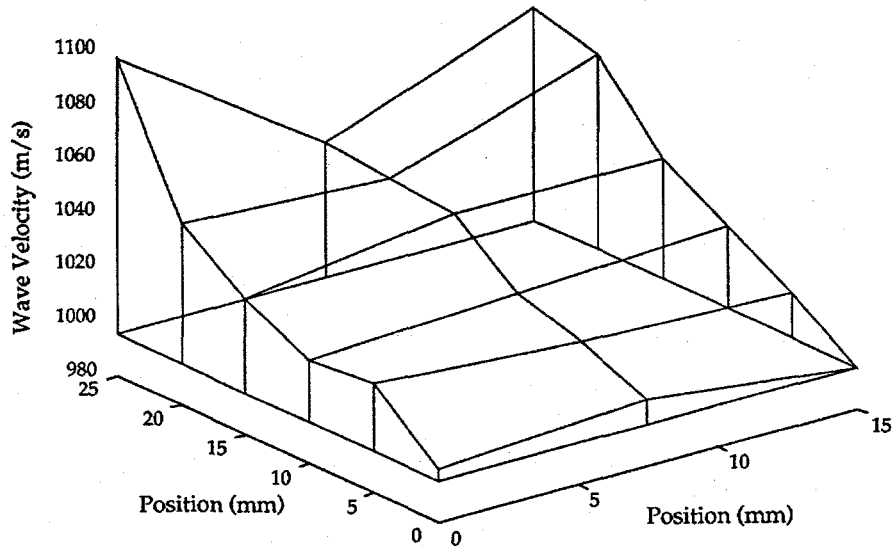


Figure 3. The surface wave velocity at various locations on a slab of alumina pressed at 68.9 MPa measured using laser ultrasonics. The front of the diagram corresponds to the bottom of the sample.

**3.4 X-ray Radiography** The x-ray radiography was performed using a Faxitron unit (Hewlett-Packard) with a voltage of 35 KV. The distance from the source to the film was 50 cm and the exposure time was varied from 2 to 10 min. Type "M" film was used. The samples were covered with a thin sheet of stainless steel to reduce scatter. Two sample thicknesses were used: 1 and 5 mm. The exposed film was scanned and then manipulated to increase the contrast using Adobe Photoshop. Other software (ImagePro Plus) was used to assign numerical values to the gray levels along a line. Densities were assigned to the gray levels using the images of the step wedges which were manipulated in identical fashion.

The radiographs of the samples indicated that the contrast due to density gradients in the thicker sample was significantly better than that in the thinner one so that only the results from it will be discussed. Figure 4 shows the results from the measurements of the image intensity along several 1 mm wide lines after using the step wedge calibration standards to convert intensity to density and after smoothing the data. In Figure 4a, the density along the edge from top to bottom is compared to that along the center line. Again, the same trends are seen. The results in Figure 4b are also consistent in showing that the density at the top decreases from edge to center whereas at the bottom the opposite happens.

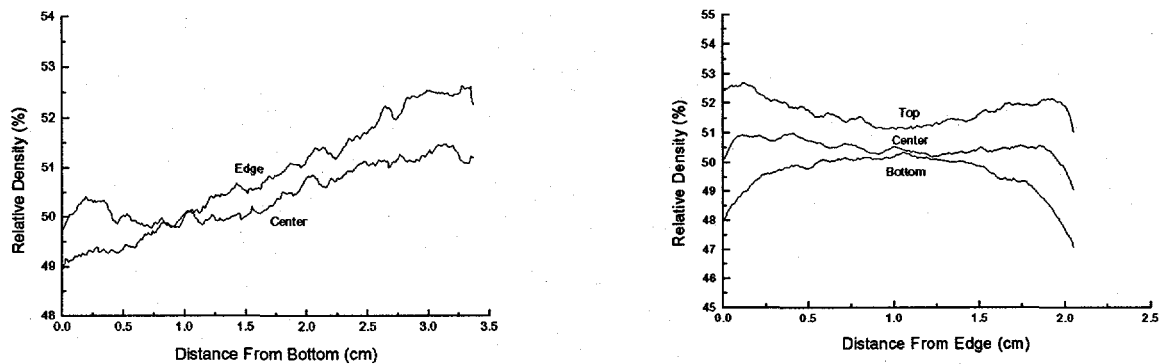


Figure 4. The density of a 5 mm thick alumina slab pressed at 68.9 MPa determined using x-ray radiography. a) The density along two 1 mm wide lines parallel to the cylinder edge, one near the edge and one near the center. b) The density along lines parallel to the top and bottom.

**3.5 Image Analysis** The sample preparation for image analysis characterization varied slightly from that described in Section 3.1. Specifically, the samples used were isopressed at 68.9 MPa (10 ksi) rather than uniaxially pressed. The results shown here are similar to those obtained in die-pressed samples. Axial slices of isopressed compacts were vacuum impregnated with epoxy, and cured under pressure in order to completely fill the porosity. This facilitates standard ceramographic techniques for these highly porous samples. Polished surfaces were then coated with a thin layer of carbon, and imaged using an Amray 1645 scanning electron microscope. Backscattered electron images were obtained at 800x using 20 kV accelerating voltage. Image processing was performed using a Tracor Northern 8500 Image Analysis system. The backscattered electron image was digitized and converted into a binary image using gray scale thresholding. The significant differences in gray scale between the alumina particles and the epoxy-infiltrated porosity provided sufficient contrast to accurately and distinctly isolate the two phases. Areal fractions of the solid alumina phase were then quantified from these binary images, taken along four radial lines from the center to the edge of the sample. In Figure 5, the measured areal fractions in terms of relative density as a function of radial position are shown.

## 4. DISCUSSION

Density gradients showing the expected trends were detected with all four techniques. The ultrasonic velocity measurements gave the best overall density gradients characterization since it produced a two dimensional contour map of the sample with good spatial resolution and the best density resolution of all the techniques. It may be possible to achieve a similar result with

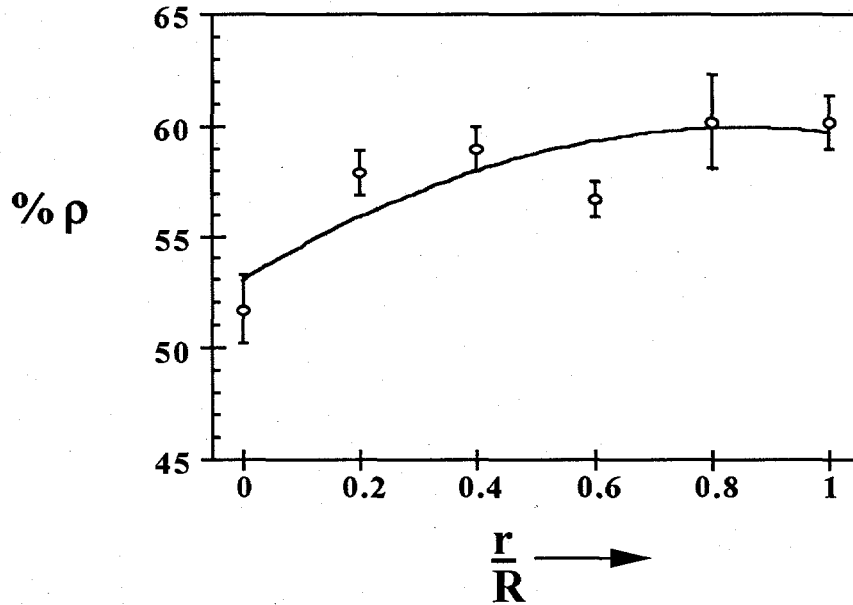


Figure 5. The measured relative densities computed by image analysis as a function of radial position, where 0 represents the center and 1 is the outer edge of the sample. Note that the density varies by approximately 8% from the center to the edge. Error bars represent the standard deviation of four images analyzed at each radial position.

laser ultrasonics with a system equipped with automated scanning capability. Although the density and spatial resolutions were not quite as good for x-ray radiography, the trends in density variation could be clearly seen. Therefore, radiography may be more suitable in settings where a large number of samples need to be characterized, since they can be done simultaneously, or where cost is an issue, since the ultrasonic system used in this work was nearly ten times the price of a Faxitron.

## 5. SUMMARY

Density gradients are known to develop during typical powder compaction processes. In this paper, several techniques were identified and shown to accurately characterize and quantify density variations in a common alumina ceramic. The experimental results derived from these techniques can be used to generate density distribution maps, that then can be used to compare compaction model predictions with actual experimental results. Such characterization techniques are important feedback tools for developing models with improved predictive capability, and enhanced process control in industrial manufacturing operations.

## Acknowledgements

This work was performed at Sandia National Laboratories, and was supported by the U.S. Department of Energy under Contract Number DE-AC04-94AL85000. The authors thank Bonnie McKenzie for performing the image analysis.

## 6. REFERENCES

1. F.M. Mahoney and M.J. Readey, Proc. of International Symposium on the Science, Technology and Commercialization of Powder Synthesis and Shape Forming Processes, American Ceramic Soc., Westerville, OH, to be published.
2. D.E. Bray and D. McBride, eds., Nondestructive Testing Techniques, John Wiley and Sons, New York, 1992, pp 253-276.
3. W. M. D. Wright, D.A. Hutchins and M.H. Lewis, J. Mat. Sci. Let., 14, 366-9 (1995).
4. M. P. Jones, G.V. Blessing and C.R. Robbins, Materials Evaluation, 44, 859-862 (1985).
5. R.A. Roberts, Mater. Eval., 46, 758-766 (1988).
6. K. Yamanaka, C.K. Jen, C. Neron and J.F. Bussière, Mater. Eval., 47, 828-834 (1989).
7. M. Oksanen, Acta Polytechnica Scandinavica, Applied Physics Series 133, 4-32 (1994).
8. M. Oksanen and M. Luukkala, Review of Progress in Quantitative Nondestructive Evaluation, Vol. 9, D.O. Thompson and D.E. Chimenti, Eds., pp. 1149-1152, Plenum Press, New York, 1990.
9. D.E. Bray and D. McBride, eds., Nondestructive Testing Techniques, John Wiley and Sons, New York, 1992, pp. 113-146.
10. H. M. MacLeod and K. Marshall, Powder Technology, 16, 107-122 (1977).
11. D.E. Bray and D. McBride, eds., Nondestructive Testing Techniques, John Wiley and Sons, New York, 1992, pp.161-184.

12. S. Rokugawa, S. Usui and B.D. Sawicka, "Nondestructive Evaluation of Ceramic Components by  $\gamma$ -Ray CT," Atomic Energy of Canada Limited Report AECL-10461, 1991.
13. W.A. Ellingson, D.L. Holloway, E.A. Sivers, J. Ling, J.P. Pollinger and H.C. Yeh, Proc. of the Annual Automotive Technology Development Contractors' Coordination Meeting, 433-437, SAE, Warrendale, PA, 1992.
14. D.E. Bray and D. McBride, eds., Nondestructive Testing Techniques, John Wiley and Sons, New York, 1992, pp. 225-250.
15. W.A. Ellingson, J.L. Ackerman, L. Garrido, J.D. Weyand and R.A. DiMilia, Ceram. Eng. Sci. Proc., **8** (7-8) 503-512 (1987).